J Therm Anal Calorim (2010) 101:339–347
DOI 10.1007/s10973-010-0749-1

The neural network and multivariate linear regression approach for observing phase transitions of polymers with the differential thermal analysis method

Murat Beken

Received: 7 July 2009 / Accepted: 11 March 2010 / Published online: 30 March 2010

Abstract The aim of this study was to correlate the results of experimental data using DTA method and predictions of artificial neural network (ANN) and multivariate linear regression (MLR). Thermal decomposition of polymers was analyzed by simultaneous DTA method, and kinetic parameters (critical points, the change of enthalpy and entropy) of polymers were investigated. A computer model based on multilayer feed forwarding back propagation and multilayer linear regression model were used for the prediction of critical points, phase transitions of low-density polyethylene (LDPE) and mid-density polyethylene. As a result of our study, we concluded that ANN model is more suitable than MLR about prediction of experimental data.

Keywords Differential thermal analysis (DTA) · Artificial neural networks (ANN) · Multivariate linear regression (MLR) · LDPE and MDPE · Phase transitions · Enthalpy · Entropy · Melting Point

Introduction

The opinion of showing the heat with curves was suggested by Le Chatelier in nineteenth century. But the idea of obtaining temperature difference (ΔT) depending on heat curves was propounded by Roberts-Austen in 1899. In 1904, the first classical "differential thermal analysis (DTA) device" was produced by Kurnakov-Saladin, and in 1952, after the development of electric appliance, Stener laid the foundations of modern DTA device. DTA devices, which are used nowadays, have been improved as a result of these works.

Differential thermal analysis is a method which is used for observing the change of energy and recording the difference between reference and sample substance. The peaks, which are obtained from DTA curves, show endothermic and exothermic reactions. Besides, knowledge about phase transitions, solid state reactions, active gas reactions can be obtained by the virtue of DTA peaks.

In this study, DTA method has been correlated with ANN and MLR, using a computer-controlled handmade DTA device, which can take measurements up to 300 atm Changes of critical temperature, entropy, and enthalpy have been analyzed under different high pressure for the solid–liquid phase transition of low-density polyethylene (LDPE) and mid-density polyethylene (MDPE). For the simulation of obtained experimental data, ANN method and MLR model have been used.

A lot of studies about application of artificial neural networks (ANNs) in DTA have taken part in the literature. Calculations of thermodynamic properties have been handled in the certain parts of these studies [1, 2]. One of these studies, which is concerned with the use of neural network approach to analyze heat transfer, has been actualized by Ayhan-Sarac and co-workers [3]. Similarly, an ANN approach has been made for heat transfer, and flow characteristics in channels with baffles have been presented [4]. The other study in the literature has been verified by Tomaszewicz and Kotfica [2]. In this study, thermal decomposition of $CoSO_4 \cdot 7H_2O$ by simultaneous DTA-TG techniques has been observed, and it was concluded that the application of neural network approach to DTA method makes possible to predict the kinetic parameters [2]. Besides, some studies based on MLR approach to the DTA

M. Beken (✉)
Applied Mathematics Department, Halic University, Bomonti, Istanbul, Turkey
e-mail: muratbeken@halic.edu.tr

remain one of the studies in the literature [5]. However, in this study, two simulation models have been combined discrepant from these studies. For this reason ANN and MLR models have been used for the simulation of experimental data. So, we have concluded that ANN has given better results than MLR.

Method

Differential thermal analysis

Differential thermal analysis is a method which comprises heating or cooling a test sample and an inert reference under identical conditions, while recording the temperature difference (ΔT) between the sample and reference material [6]. Then this temperature difference is plotted against time, or against temperature. Changes in the sample, which trigger the absorption or evolution of heat, can be detected relative to the inert reference. Apart from these situations, DTA can be used to study thermal properties and phase transitions.

Structure of DTA

The DTA device used in the experiment is composed of three main partitions (see Fig. 1).

Heating block: A cylinder-shaped copper mass, which conducts heat, includes the Alumina-Oxide holders for the sample and the reference materials. The linearly increasing temperatures of these holders are obtained with a PID-controller. NiCr–Ni thermocouples (type K) of 1 mm diameter are used for the temperature measurement. The thermal emf of this type of thermocouples is nearly independent of pressure in the range 0.1–300 atm [7]. After Rittmeier-Kettner the influence of pressure on the emf should be smaller than 0.2 K below 1,000 MPa [8]. Furthermore the thermo wires are not in direct contact with the pressurized gas but are shielded with an inconel mantle also reducing the effect of pressure. To verify that the emf is practically independent of pressure up to 300 atm, the melting point of indium was measured and compared with melting point data of the literature [9, 10]. For temperature calibration the following substances were used:

- Indium (154.8 °C)
- Benzoic acid (122.6 °C)

The dependence of the emf on temperature was assumed to be linear. The standard deviation after repeated determination of the melting point of indium was found to be °C.

DTA processing unit: The data obtained from these measurements are collected by a Data Logger with Analog/Digital and Digital/Analog converters. These collected data are stored and processed in a PC, and a printer is used to transfer these data to a paper form. In addition, these pressure valves, for the gas flow, were controlled by the values of the pressure transmitters.

Pressure unit: DTA pressure unit consists of a couple of piston and a valve of nitrogen gas. Also a pressure converter is used to reach high pressure. So the different diameters of the pistons with constant pressure force can provide different pressure values in two different pressure rooms.

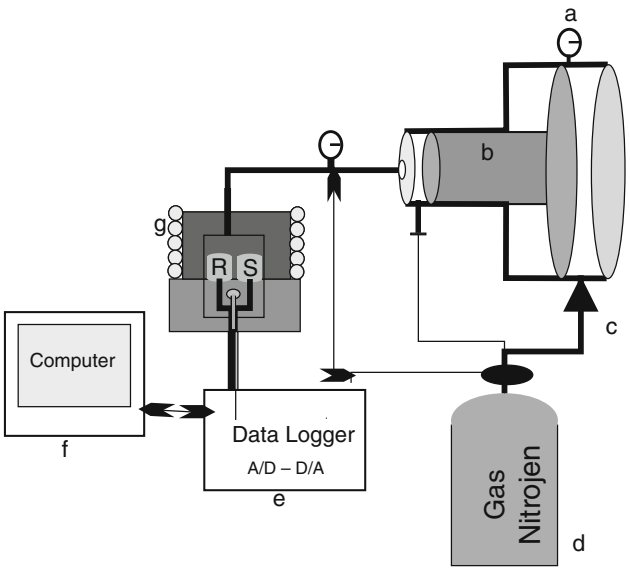

Fig. 1 Scheme of the installation: *a* Digital barometer (pressure transmitter); *b* pressure unit; *c* control sensor valve; *d* gas bottles; *e* data logger (D/A–A/D); *f* computer; *g* Heater-heating block

ANN modeling

ANNs were developed in the attempt of simulating the biological nervous systems in learning information from the outside environment [11]. They consist of simple synchronous processing elements, which are inspired by biological neural networks. Scientists improved ANNs based on the ability of apprehending difficult and complex samples of the brain [12].

ANN is frequently favored method because of easy applicability and not requiring too many data. Classic computing systems can be affected easily and do not work if a data lacking is in question. However, it is not comprehensive for ANNs. A good training network, which has the ability of high generalization capacity, can continue activity of decision making. In this situation, performance of the system can decrease but it does not reach the point of stop [13].

A lot of learning algorithms have been developed in the process of development of ANN. One of the most common and successful algorithms is multilayer feedforward backpropagation, also called multilayer perceptrons (MLP). Feedforward backpropagation method of artificial neural is the commonly used method. In this method, network has three layers which are named as input layer, output layer, and hidden layer. Every unit is composed of a great deal of neurons and the connections take over between these neurons. Feedforward backpropagation method consists of two stages: One of them transmits the input signal forwardly to calculate the output signal in the output unit. Second one assigns the weights based on the differences between signals which are observed and calculated in the output unit. So learning algorithm changes the weights for every iteration until the training puts across [14].

Feedforward neural networks are ideally suitable for modeling relationships between a set of predictor or input variables and one or more response or output variables. For this reason, we will focus more on feedforward networks in this study.

MLR modeling

In statistics, linear regression refers to any approach to modeling the relationship between one or more response variables denoted y and one or more independent variables denoted x. This model depends linearly on the unknown parameters to be estimated from the data. Such a model is called a linear model [15]. Most commonly, linear regression refers to a model in which the conditional mean is an affine function of x. Like all forms of regression analysis, linear regression focuses on the conditional probability distribution of given x, rather than on the joint probability distribution of y and x, which is the domain of multivariate analysis. Linear regression has many practical uses. One of them is to fit a predictive model to an observed data set of y and x values. After developing such a model, if an additional value of x is then given without its accompanying value of y, the fitted model can be used to make a prediction of the value of y. For this reason, MLR model has been used for making predictions and forecasting besides ANN model.

Experimental

DTA measurements

High pressure DTA

The thermal behaviors of MDPE and LDPE were examined under hydrostatic pressures up to 250 atm by using an HP-DTA apparatus. The sample covered by aluminum foil, which was fixed onto an NiCrNi thermocouples (type K) junction, by giving it a coating with an epoxy adhesive. The temperature and the heat of transition were calibrated with an Indium and Benzoic acid at given pressures: the accuracy of the observed enthalpy of transition was estimated to be %10. The transition temperatures were examined at the maxima of the exothermic and endothermic peaks in these HP-DTA measurements.

Clapeyron relation

The entropy changes at the phase transition can be alternatively estimated with the aid of the Clasius–Clapeyron relation:

$$\Delta S_{\mathrm{tr}} = \Delta H_{\mathrm{tr}}/T_{\mathrm{tr}} = \Delta V_{\mathrm{tr}}\mathrm{d}P/\mathrm{d}t \quad (1)$$

The transition enthalpies and entropies estimated from Eq. 1 at $P = 1$, 20, 50, 80, 100, 125, 150, 175, 200, 250 atm for LDPE and MDPE are summarized in Tables 1 and 2. For this reason, ΔH_{tr} was calculated by using calibration constant and the peak areas of DTA. Antecedently, ΔS_{tr} was obtained from the values of ΔH_{tr} and Eq. 1.

ANN simulation

In this study, an ANN training program, whose computational stencil bases on multilayer feedforward backpropagation method, was used to compare the experimental data and output values of neural network. For this purpose, training sets were composed of our experimental data. Input sets were composed of Pressure (atm), Heating rate (°C min^{-1}), and Mass (kg). Experimental data of DTA curve area (mW), Melting point (°C), the change of the Enthalpy (J kg^{-1}), and Entropy (J kg^{-1} $^{\circ}\mathrm{C}^{-1}$) were used as output set (see Fig. 2).

However, input and output values, which were used as the training set, were normalized thereby converting real numbers between 0 and 1 to train the kinetic parameters correctly and obtain consistent results.

In the first training processing of MDPE, we stabilized the momentum rate as 0.9 and iteration number as 10,000 prelusively. Hidden layer number was chosen as 1 and the elements of it were chosen as 4. We observed which learning rate provides the best results by changing the learning rate between 0 and 1. As can be seen from the Fig. 3 when the learning rate had reached to 0.9, minimum error rate was obtained.

At this point, we changed momentum rate between 0 and 1, for the learning rate which provides the best results at the previous step. Iteration number was chosen as 10,000. The system was trained until target values had been

Table 1 The enthalpy, entropy, and critical temperature values of MDPE under different pressure values

P/atm	Q/°C min^{-1}	m/kg	DH area/mW	ΔH/J kg^{-1}	$T_{melting}$/°C	ΔS/J kg^{-1} °C^{-1}
1	7.90	$0.0429 \cdot 10^{-3}$	7504.00	$153.06 \cdot 10^{3}$	126.45	1208.01
20	7.90	$0.0429 \cdot 10^{-3}$	7109.00	$144.72 \cdot 10^{3}$	127.70	1132.22
50	8.27	$0.0232 \cdot 10^{-3}$	3501.99	$138.23 \cdot 10^{3}$	129.22	1067.46
75	8.56	$0.0232 \cdot 10^{-3}$	3012.73	$127.40 \cdot 10^{3}$	130.90	975.58
80	8.56	$0.0289 \cdot 10^{-3}$	3800.36	$123.77 \cdot 10^{3}$	131.40	944.62
100	8.92	$0.0308 \cdot 10^{-3}$	3601.91	$115.57 \cdot 10^{3}$	132.70	874.00
120	7.86	$0.0277 \cdot 10^{-3}$	3454.40	$107.50 \cdot 10^{3}$	134.60	797.11
125	7.86	$0.0277 \cdot 10^{-3}$	3385.00	$105.60 \cdot 10^{3}$	134.90	781.07
150	7.55	$0.0284 \cdot 10^{-3}$	3324.98	$96.30 \cdot 10^{3}$	137.06	701.16
160	7.55	$0.0277 \cdot 10^{-3}$	3086.40	$93.14 \cdot 10^{3}$	137.10	675.92
175	7.55	$0.0277 \cdot 10^{-3}$	2893.52	$88.39 \cdot 10^{3}$	138.90	634.29
180	7.72	$0.0232 \cdot 10^{-3}$	2186.30	$88.10 \cdot 10^{3}$	139.20	632.06
200	7.86	$0.0256 \cdot 10^{-3}$	2192.55	$81.80 \cdot 10^{3}$	140.70	581.32
240	7.95	$0.0277 \cdot 10^{-3}$	1992.20	$71.00 \cdot 10^{3}$	143.80	494.54
250	7.95	$0.0271 \cdot 10^{-3}$	1839.44	$68.71 \cdot 10^{3}$	144.60	476.16

Table 2 The enthalpy, entropy and critical temperature values of LDPE under different pressure values

P/atm	Q/°C min^{-1}	m/kg	DH area/mW	ΔH/J kg^{-1}	$T_{melting}$/°C	ΔS/J kg^{-1} °C^{-1}
1	7.75	$0.0151 \cdot 10^{-3}$	2208.80	$125.20 \cdot 10^{3}$	129.10	969.70
20	7.75	$0.0150 \cdot 10^{-3}$	2649.50	$119.76 \cdot 10^{3}$	129.30	960.70
50	8.84	$0.0150 \cdot 10^{-3}$	1701.20	$110.76 \cdot 10^{3}$	129.90	854.20
75	8.79	$0.0152 \cdot 10^{-3}$	2090.20	$104.82 \cdot 10^{3}$	130.10	805.40
80	8.84	$0.0150 \cdot 10^{-3}$	2076.43	$103.76 \cdot 10^{3}$	130.50	794.70
100	8.95	$0.0151 \cdot 10^{-3}$	2050.02	$99.61 \cdot 10^{3}$	131.00	760.00
120	8.95	$0.0162 \cdot 10^{-3}$	2076.72	$97.44 \cdot 10^{3}$	131.50	740.50
125	8.84	$0.0156 \cdot 10^{-3}$	1544.99	$96.95 \cdot 10^{3}$	131.60	736.60
150	8.84	$0.0161 \cdot 10^{-3}$	1737.76	$95.06 \cdot 10^{3}$	132.30	718.50
160	8.95	$0.0152 \cdot 10^{-3}$	1472.01	$94.93 \cdot 10^{3}$	132.60	715.90
175	8.56	$0.0154 \cdot 10^{-3}$	1526.07	$94.85 \cdot 10^{3}$	132.80	713.70
180	8.78	$0.0162 \cdot 10^{-3}$	1575.10	$94.53 \cdot 10^{3}$	133.20	709.70
200	8.84	$0.0162 \cdot 10^{-3}$	1551.16	$93.73 \cdot 10^{3}$	134.10	698.90
240	8.84	$0.0158 \cdot 10^{-3}$	1504.11	$93.21 \cdot 10^{3}$	135.70	686.70
250	8.84	$0.0156 \cdot 10^{-3}$	1484.76	$93.19 \cdot 10^{3}$	136.10	684.50

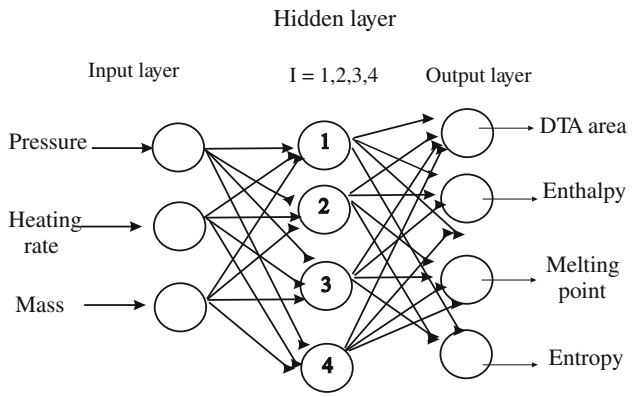

Fig. 2 Diagram illustrating a simple 3-4-4 neural network

obtained. It was concluded that minimum error rate was obtained when the momentum rate reached 0.9 (see Fig. 4).

At the next phase, both of learning and momentum rates were selected as 0.9. Iteration number was changed between 1,000 and 10,000. When it was observed that the best results had been obtained, the system was stopped and the outputs of the neural networks were recorded. As can be seen from the Fig. 5, the best results have been obtained when the iteration number reached 10,000.

Validation sets have been used to determine when to stop train the network for avoiding overtraining. Then, test

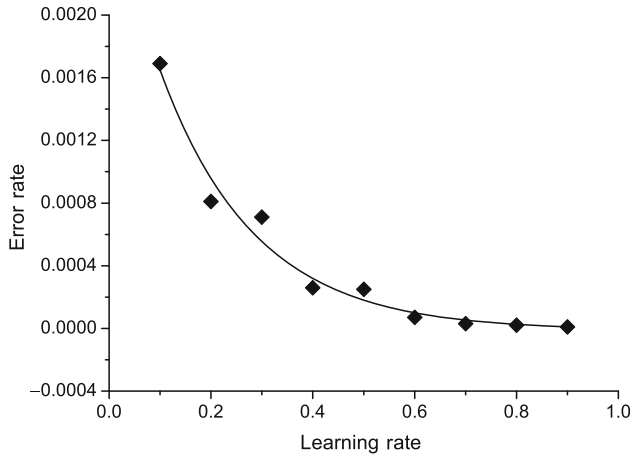

Fig. 3 The change of error rate depending on learning rate for MDPE

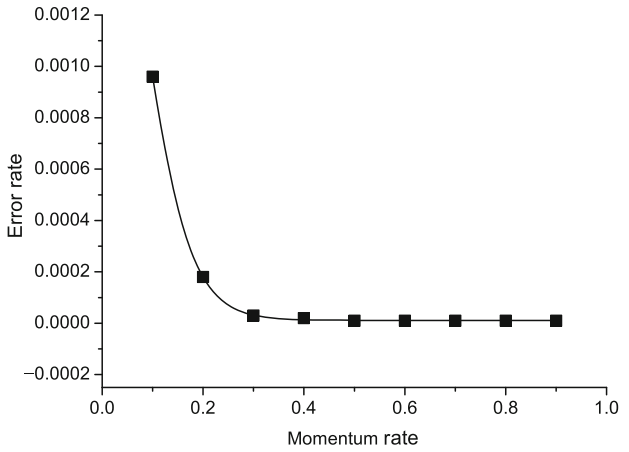

Fig. 4 The change of error rate depending on momentum rate for MDPE

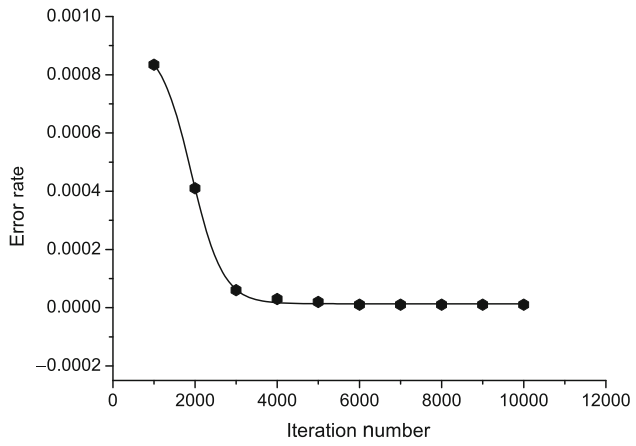

Fig. 5 The change of error rate depending on iteration number for MDPE

sets have been composed of the experimental data, which have not been used for training the network for checking the achieved predictive ability of ANN. As can be seen from the Table 3, we used experimental data, which have been obtained at the end of the measurements under 75, 120, 160, 180, and 240 atm pressure. Although these input values had not been used for training the network, the system created the approximate values to the experimental data.

The same transactions of ANN prediction were actualized for LDPE. Previously, hidden layer number was chosen as 1 and the number of neurons for hidden layer was specified as 4. One of the momentum rate, learning rate, and iteration number were kept constant alternately and it was observed how the other elements affect the system. As can be seen from the Fig. 6, in the first step, momentum rate was changed between 0 and 1, learning rate was chosen 0.8 and iteration number was selected as 5,000. For every momentum rate, the outputs of the neural network were recorded. It was seen that the minimum error rate was obtained when the momentum rate was 0.8.

After determining the momentum rate, which creates the minimum error, it was kept constant and iteration number was chosen as 5000 again. In the present instance, learning rate was manipulated between 0 and 1. Obtained error rate was recorded for every learning rate. As can be seen above, the best results were obtained for 0.8 learning number (Fig. 7).

In the next step, momentum and learning coefficients were kept constant. In this step, momentum rate and learning rate, which create the best results in the previous steps, were used. The iteration number was changed between 1,000 and 10,000. As can be seen from the Fig. 8, the best results had been obtained when the iteration number reached 10,000.

Besides validation, test sets have been composed of the experimental data, which have not been used for training the network for checking whether the network created satisfactory results at the end of simulation. It has been observed that the system created the approximate values to the experimental data although these input values had not been used for training the network (see Table 4).

MLR simulation

In this study MLR Modeling has been chosen as second simulation method. For understanding how prediction could be made in MLR equations must be examined (Figs. 9, 10, 11 and 12). In a given data set of n statistical units, a linear regression model assumes that the $(y_i; x_{i,1}; x_{i,2}; \ldots; x_{i,k})_i'$ relationship between the response variable y_i and the p-vector of regressors x_i independent variables. Thus the model takes the form

Table 3 The experimental and neural network output values for MDPE

Input values			Output values							
P/atm	Q/°C min^{-1}	m/kg	DH area/mW		ΔH/J kg^{-1}		T_{melting}/°C		ΔS/J kg^{-1} °C^{-1}	
E	E	E	E	N	E	N	E	N	E	N
75	8.56	$0.0232 \cdot 10^{-3}$	3012.73	2997.94	$127.40 \cdot 10^{3}$	$127.60 \cdot 10^{3}$	130.90	130.87	975.12	975.00
120	7.86	$0.0277 \cdot 10^{-3}$	3454.40	3456.55	$107.50 \cdot 10^{3}$	$107.31 \cdot 10^{3}$	134.60	134.58	797.78	797.16
160	7.55	$0.0277 \cdot 10^{-3}$	3086.40	3086.47	$93.14 \cdot 10^{3}$	$92.98 \cdot 10^{3}$	137.10	137.26	675.01	674.64
180	7.72	$0.0232 \cdot 10^{-3}$	2186.30	2178.56	$88.10 \cdot 10^{3}$	$88.06 \cdot 10^{3}$	139.20	139.12	632.26	632.62
240	7.95	$0.0277 \cdot 10^{-3}$	1992.20	1994.39	$71.00 \cdot 10^{3}$	$71.02 \cdot 10^{3}$	143.80	143.87	494.04	494.14

E experimental values, *N* neural network output values

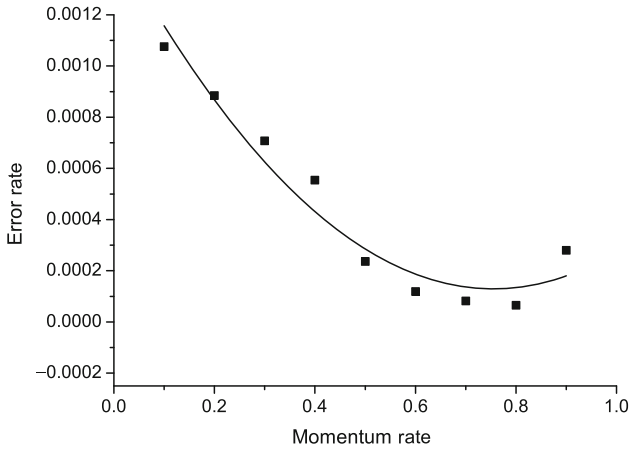

Fig. 6 The change of error rate depending on momentum rate for LDPE

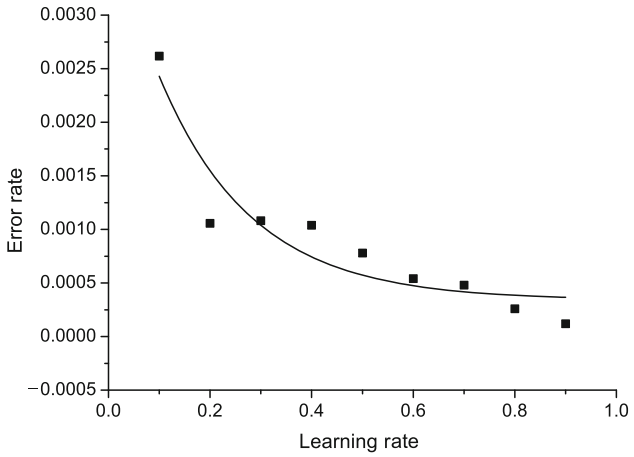

Fig. 7 The change of error rate depending on learning rate for LDPE

$$y_i = \beta_0 + \beta_1 x_{i,1} + \beta_2 x_{i,2} + \cdots + \beta_k x_{1,k} + \epsilon_i = \sum_{i=1}^{n} x_i' \beta + \epsilon_i \tag{2}$$

After determining the regression coefficients, it is theorically possible to find new y values for other x inputs.

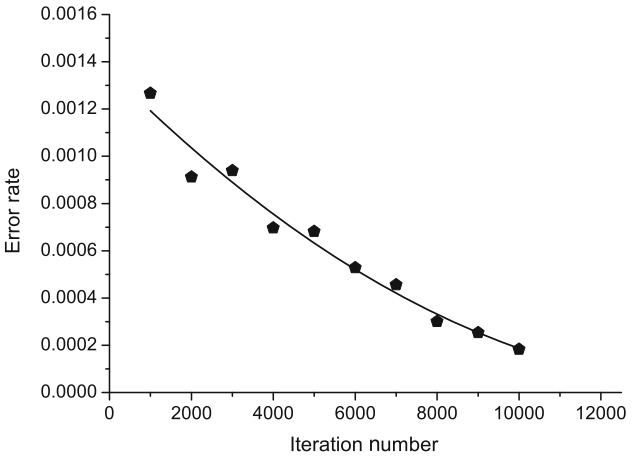

Fig. 8 The change of error rate depending on iteration number for LDPE

In this method, m equations are stacked together and written in vector form as

$$\mathbf{y_i} = \begin{pmatrix} y_{i_1} \\ y_{i_2} \\ \vdots \\ y_{i_m} \end{pmatrix} \tag{3}$$

and p-vector of regressors can be defined as a matrix

$$\mathbf{x} = \begin{pmatrix} x_1' \\ x_2' \\ x_3' \\ \vdots \\ x_n' \end{pmatrix} = \begin{pmatrix} x_{11} & x_{12} & \ldots & x_{1p} \\ x_{21} & x_{22} & \ldots & x_{2p} \\ \vdots & \vdots & \ddots & \vdots \\ x_{n_1} & \ldots & \ldots & x_{np} \end{pmatrix} \tag{4}$$

So regression coefficients can be calculated by the method of least squares. The ordinary least squares estimates β are found in a manner analogous to the univariate case we begin by collecting the univariate least squares estimates yields

$$\beta = [\beta_1 | \beta_2 | \cdots | \beta_m] = (z'z)z'y = [y_1 | y_2 | \cdots | y_m] \tag{5}$$

Table 4 The experimental and neural network output values for LDPE

Input values			Output values							
P/atm	Q/°C min^{-1}	m/kg	DH area/mW		ΔH/J kg^{-1}		$T_{melting}$/°C		ΔS/J kg^{-1}	
E	E	E	E	N	E	N	E	N	E	N
75	8.84	$0.0152 \cdot 10^{-3}$	2090.00	2108.03	$104.80 \cdot 10^{3}$	$104.26 \cdot 10^{3}$	130.10	130.87	805.4	801.50
120	8.95	$0.0162 \cdot 10^{-3}$	2076.00	2068.50	$97.43 \cdot 10^{3}$	$99.03 \cdot 10^{3}$	131.50	134.35	740.5	747.60
160	8.95	$0.0152 \cdot 10^{-3}$	1472.00	1439.55	$94.53 \cdot 10^{3}$	$94.17 \cdot 10^{3}$	132.60	133.98	715.9	728.30
180	8.78	$0.0162 \cdot 10^{-3}$	1575.80	1551.18	$94.37 \cdot 10^{3}$	$93.14 \cdot 10^{3}$	133.20	134.12	709.7	707.60
240	8.84	$0.0158 \cdot 10^{-3}$	1504.00	1492.01	$93.21 \cdot 10^{3}$	$94.24 \cdot 10^{3}$	135.70	134.55	686.7	678.90

E experimental values, *N* neural network output values

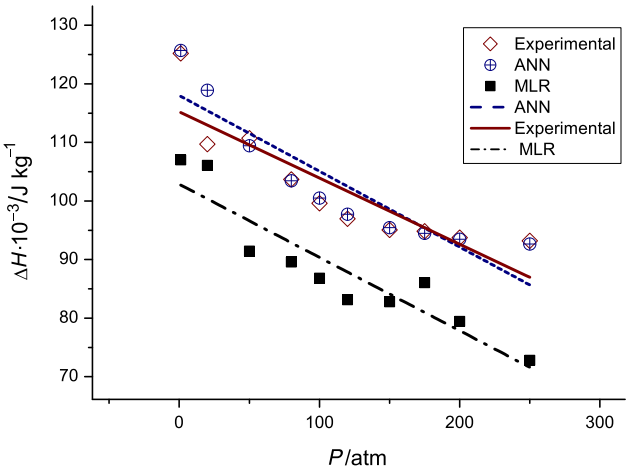

Fig. 9 The change of enthalpy depending on pressure for LDPE

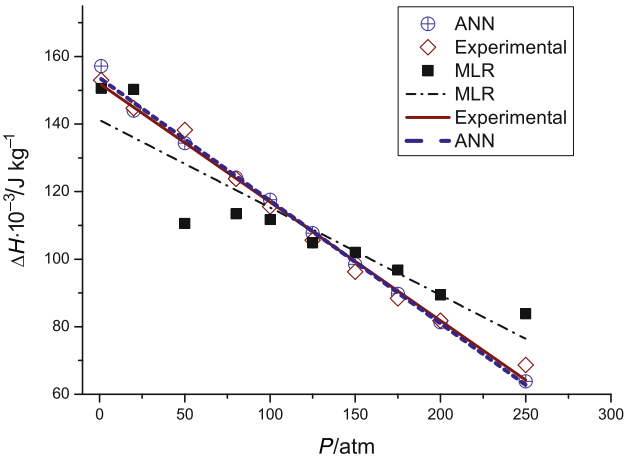

Fig. 11 The change of enthalpy depending on pressure for MDPE

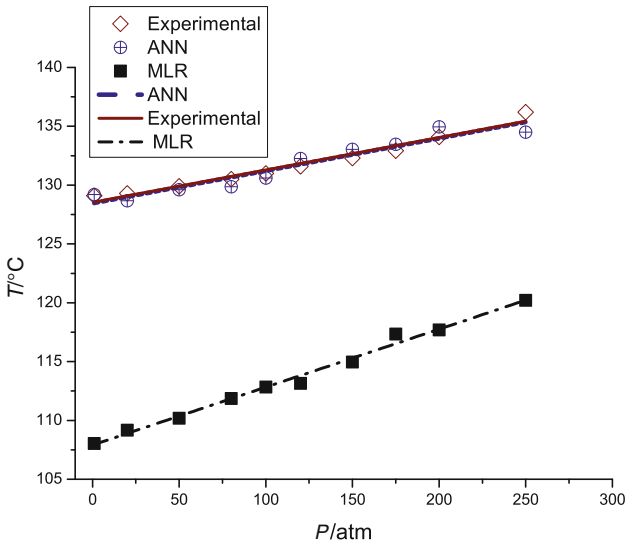

Fig. 10 The change of critical temperature depending on pressure for LDPE

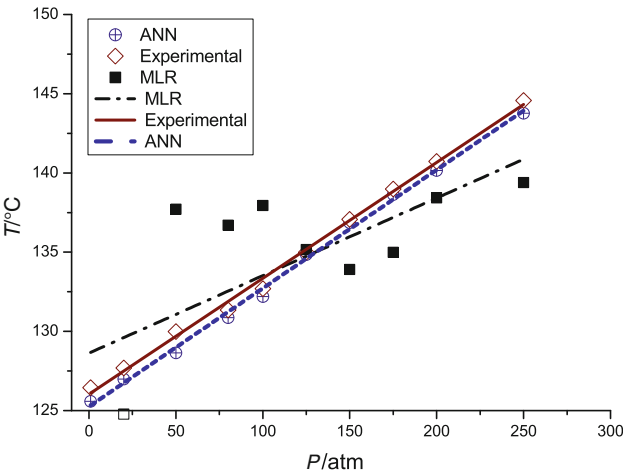

Fig. 12 The change of critical temperature depending on pressure for MDPE

Table 5 The experimental, MLR, and neural network output values for MDPE

Input values			Output values											
P/atm	Q/°C min^{-1}	m/kg	DH area/mW			ΔH/J kg^{-1}			$T_{melting}$/°C			ΔS/J kg^{-1} °C^{-1}		
E	E	E	E	N	M	E	N	M	E	N	M	E	N	M
1	7.90	$0.0429 \cdot 10^{-3}$	7504.00	7496.54	7484.52	$153.06 \cdot 10^{3}$	$150.56 \cdot 10^{3}$	$157.15 \cdot 10^{3}$	126.45	125.59	123.54	1208.01	1237.58	1184.55
20	7.90	$0.0414 \cdot 10^{-3}$	7109.00	7103.00	7014.00	$144.72 \cdot 10^{3}$	$143.95 \cdot 10^{3}$	$150.33 \cdot 10^{3}$	127.70	126.99	124.78	1132.22	1126.00	1176.96
50	8.27	$0.0232 \cdot 10^{-3}$	3501.99	3550.40	3389.41	$138.23 \cdot 10^{3}$	$134.37 \cdot 10^{3}$	$110.61 \cdot 10^{3}$	129.22	128.64	137.71	1067.46	1029.85	831.38
80	8.56	$0.0289 \cdot 10^{-3}$	3800.36	3829.11	3803.79	$123.77 \cdot 10^{3}$	$124.12 \cdot 10^{3}$	$113.41 \cdot 10^{3}$	131.40	130.86	136.71	944.62	948.90	859.80
100	8.92	$0.0308 \cdot 10^{-3}$	3601.91	3625.70	3672.55	$115.57 \cdot 10^{3}$	$117.57 \cdot 10^{3}$	$111.78 \cdot 10^{3}$	132.70	132.20	137.94	874.00	896.00	849.60
125	7.86	$0.0270 \cdot 10^{-3}$	3385.00	3383.81	3430.22	$105.60 \cdot 10^{3}$	$104.80 \cdot 10^{3}$	$107.72 \cdot 10^{3}$	134.90	134.84	135.17	781.07	778.60	803.90
150	7.55	$0.0284 \cdot 10^{-3}$	3324.98	3305.08	3401.40	$96.30 \cdot 10^{3}$	$98.52 \cdot 10^{3}$	$102.09 \cdot 10^{3}$	137.06	136.86	133.90	701.16	724.60	752.80
175	7.55	$0.0277 \cdot 10^{-3}$	2893.52	2874.40	2968.74	$88.39 \cdot 10^{3}$	$89.72 \cdot 10^{3}$	$96.78 \cdot 10^{3}$	138.90	138.63	134.99	634.29	648.70	707.60
200	7.86	$0.0256 \cdot 10^{-3}$	2192.55	2198.93	2132.26	$81.80 \cdot 10^{3}$	$81.32 \cdot 10^{3}$	$89.41 \cdot 10^{3}$	140.70	140.16	138.43	581.32	576.50	647.17
250	7.95	$0.0271 \cdot 10^{-3}$	1839.44	1846.25	1702.11	$68.71 \cdot 10^{3}$	$63.81 \cdot 10^{3}$	$83.84 \cdot 10^{3}$	144.60	143.76	139.39	476.16	428.70	601.10

E experimental values, *N* neural network output values, *MLR* multivariate linear regression outputs

Table 6 The experimental and neural network output values for LDPE

Input values			Output values											
P/atm	Q/°C min^{-1}	m/kg	DH area/mW			ΔH/J kg^{-1}			$T_{melting}$/°C			ΔS/J kg^{-1} °C^{-1}		
E	E	E	E	N	M	E	N	M	E	N	M	E	N	M
1	7.75	$0.0151 \cdot 10^{-3}$	2208.80	2294.98	2120.25	$125.20 \cdot 10^{3}$	$125.71 \cdot 10^{3}$	$107.04 \cdot 10^{3}$	129.10	129.19	108.04	969.70	974.30	849.60
20	7.75	$0.0150 \cdot 10^{-3}$	2649.50	2743.00	2111.00	$119.76 \cdot 10^{3}$	$118.90 \cdot 10^{3}$	$106.08 \cdot 10^{3}$	129.30	128.67	109.18	960.70	956.80	839.20
50	8.84	$0.0150 \cdot 10^{-3}$	1701.20	1805.10	1703.09	$110.76 \cdot 10^{3}$	$109.43 \cdot 10^{3}$	$91.47 \cdot 10^{3}$	129.90	129.60	110.19	854.20	851.00	706.90
80	8.84	$0.0150 \cdot 10^{-3}$	2076.43	2113.98	1660.45	$103.76 \cdot 10^{3}$	$103.47 \cdot 10^{3}$	$89.60 \cdot 10^{3}$	130.50	129.86	111.86	794.70	791.80	687.60
100	8.94	$0.0151 \cdot 10^{-3}$	2050.02	2041.06	1576.75	$99.61 \cdot 10^{3}$	$100.49 \cdot 10^{3}$	$86.84 \cdot 10^{3}$	131.00	130.59	112.83	760.00	757.90	661.60
125	8.95	$0.0156 \cdot 10^{-3}$	1544.99	1738.36	1346.50	$97.44 \cdot 10^{3}$	$97.73 \cdot 10^{3}$	$83.16 \cdot 10^{3}$	131.60	132.27	113.16	736.60	738.90	629.40
150	8.84	$0.0161 \cdot 10^{-3}$	1737.76	1688.17	1359.12	$95.06 \cdot 10^{3}$	$95.44 \cdot 10^{3}$	$82.79 \cdot 10^{3}$	132.30	133.04	114.97	718.50	717.60	623.20
175	8.56	$0.0154 \cdot 10^{-3}$	1526.07	1666.18	1545.99	$94.85 \cdot 10^{3}$	$94.48 \cdot 10^{3}$	$86.04 \cdot 10^{3}$	132.80	133.47	117.34	713.70	713.70	648.40
200	8.84	$0.0162 \cdot 10^{-3}$	1551.16	1523.47	1269.69	$93.73 \cdot 10^{3}$	$93.49 \cdot 10^{3}$	$79.44 \cdot 10^{3}$	134.10	134.95	117.69	698.90	694.70	589.20
250	8.84	$0.0156 \cdot 10^{-3}$	1484.76	1456.34	1286.22	$93.19 \cdot 10^{3}$	$92.67 \cdot 10^{3}$	$72.83 \cdot 10^{3}$	136.10	134.50	120.20	684.50	684.80	570.40

E experimental values, *N* neural network output values, *MLR* multivariate linear regression outputs

and regression coefficients matrix can be composed of using Eq. 5 as can be seen below:

$$\mathbf{x} = \begin{pmatrix} \beta'_1 \\ \beta'_2 \\ \beta'_3 \\ \vdots \\ \beta'_n \end{pmatrix} = \begin{pmatrix} \beta_{11} & \beta_{12} & \cdots & \beta_{1p} \\ \beta_{21} & \beta_{22} & \cdots & \beta_{2p} \\ \vdots & \vdots & \ddots & \vdots \\ \beta_{n1} & \cdots & \cdots & \beta_{np} \end{pmatrix} \tag{6}$$

$$y' = x\beta' \tag{7}$$

and error matrix can be calculated by using Eq. 8:

$$\epsilon = y' - y \tag{8}$$

Conclusions

Thermodynamic and kinetic parameters could be predicted by different methods. In this study, thermal decompositions of MDPE and LDPE were predicted by using both the ANN and MLR models. Comparisons have been made for ANN and MLR models outputs against experimental values. Table 5 shows the relation between $P/\text{atm} - T/^{\circ}\text{C}, P/\text{atm} - \Delta H/\text{J}\,\text{kg}^{-1}$ for experimental and simulation data for MDPE. Also Table 6 shows the relation between $P/\text{atm} - T/^{\circ}\text{C}, P/\text{atm} - \Delta H/\text{J}\,\text{kg}^{-1}$ for experimental and simulation data for LDPE.

These observations clearly show that the neural network model is the more satisfactory approach for kinetic analysis of thermal decompositions of polymeric materials than MLR. The obtained results proved that generalization is successful enough when the network is trained correctly. But it is important to keep the number of iteration as low as possible for avoiding the overtraining of the Neural Network.

In sum, in this study, an ANN which consists of ten training data, was trained for predicting the critical points, the change of enthalpy and entropy. The samples belonging to the test set, not involved in the training process at all, indicated the real predictive ability of model. The collected data, which have been obtained from ANN, are very promising and encourage us in the use of neural networks for decomposition of polymers. In a more simple way, application of neural networks makes possible obtaining very good reproducibility of DTA experimental data.

Acknowledgements The author wishes to thank Dr. Reha Basaran for the support of experimental studies and Ozlem Ilgun for neural network studies and Derya Kosucuoglu for the support of MLR studies. Also the author wishes to thank Emirhan Emre for his technical support.

References

1. Sebastiao RCO, Braga JP, Yoshida MI. Competition between kinetic models in thermal decomposition analysis by artificial neural network. Thermochim Acta. 2004. doi:10.1016/j.tca.2003.09.009.
2. Tomaszewicz E, Kotfica M. Application of neural networks in analysis of thermal decomposition of $CoSO_4$. J Therm Anal Calorim. 2003. doi:10.1023/B:JTAN.0000005197.33066.f5.
3. Ayhan-Sarac B. Neural network methodology for heat transfer enhancement data. Int J Numer Methods Heat Fluid Flow. 2007. doi:10.1108/09615307108257774.
4. Ayhan T, Karlik B, Tandiroglu A. Flow geometry optimization of channels with baffels using neural networks and second-low of thermodynamics. Comput Mech. 2004. doi:10.1007/s00466-003-0509-1.
5. Browna ME, Maciejewskib M, Vyazovkinc S, Nomend R, Sempered J, Burnhame A, Opfermannf J, Streyg R, Andersong HL, Kemmlerg A, Keuleersh R, Janssensh J, Desseynh HO, Lii CR, Tangi TB, Roduitj B, Malekk J, Mitsuhashil T. Computational aspects of kinetic analysis part A: the ICTAC kinetics project-data, methods and results. Thermochim Acta. 2000. doi:10.1016/S0040-6031(00)00443-3.
6. Beken M. Developing differential thermal analysis device under high pressure. PhD Thesis, Yildiz Technical University; 2002.
7. Bundy FP. Effect of pressure on emf of thermocouples. J Appl Phys. 1960. doi:10.1063/1.1708993.
8. Michalik K, Drzazga Z, Michnik A, Kaszuba M. Differential scanning microcalorimetry study of thermal stability of nevirapine and azidothymidine mixture. J Therm Anal Calorim. 2006. doi:10.1007/s10973-005-7171-0.
9. Richter PW, Clarke JB. Asymmetrical friction in a piston-cylinder device and the effect on the melting curves of indium and bismuth. Rev Sci Instrum. 1980. doi:10.1063/1.1136354.
10. Sozen A, Arcaklioglu E, Ozalp M. A new approach to thermodynamic analysis of ejectorabsorption cycle: artificial neural networks. Appl Therm Eng. 2003. doi:10.1016/S1359-4311(03)00034-6.
11. Haykin S. Neural networks: A comprehensive foundation, 2–3. Englewood Cliffs: Macmillan College Publishing Company; 1994.
12. Caballero JA, Conesa JA, Font R, Marcilla A. Pyrolysis kinetics of almond shells and olive stones considering their organic fractions. J Anal Appl Pyrol. 1997. doi:10.1016/S0165-2370(97)00015-6.
13. Karlik B. Myoeletric control of multifunction prothesis using neural networks. PhD Thesis, Yildiz Technical University; 1994.
14. Maimon OZ, Rokach L. Data mining and knowledge discovery handbook. New York: Springer; 2005.
15. Brillinger DR. The identification of a particular nonlinear time series system. Biometrika. 1977. doi:10.1093/biomet/64.3.509.